Sub-Threshold Auditory-Visual Interactions in the Rat Superior Colliculus:

Linearity and Independence of EPSP Summation

10,580 words inclusive of figures and references

Abstract

The mammalian superior colliculus maintains topographic maps of visual, auditory, and somatosensory space that are in spatial alignment with eachother. The alignment of receptive fields across different modalities for neurons in the different layers of the superior colliculus, and their interconnection with eachother and with premotor nuclei, along with the presence of many cells with bi-modal and tri-modal response properties is widely thought to play an essential role in organising orienting movements of the eyes, head, and ears to stimuli across multiple modalities. It is known that the visual projection from the retina is coarsely topographic from birth, and is refined through experience-dependent processes. The auditory map, however, must be computed from non-spatial sensory signals, and its topography is disturbed following visual deprivation or visual disturbances during development. It is thus believed that visual experience in early life guides the formation of the auditory topography through multi-sensory perceptual experience. Despite the importance of understanding the mechanism of visual guidance of the auditory map, the cellular and molecular substrates of this process are unknown. We have studied the sub-threshold integration of auditory and visual excitatory post-synaptic potentials (EPSPs) in a putative cellular substrate of this visual-auditory interaction, the layer IV multi-sensory cells of the rat superior colliculus. Linear summation of EPSPs was found for coincidental stimulation of auditory and visual projections onto the same deep layer cells. Furthermore, temporal separation of auditory and visual stimulation had no effect on the synaptic integration of these signals. In most cases, average EPSP amplitude was not different from that expected from the arithmetic sum of individual responses. It is concluded either that the mechanisms of auditory-visual guidance involve a supra-threshold component, such as long-term potentiation of coincidentally active synapses, or that the primary site of auditory-visual interaction is at an earlier processing stage in the inferior colliculus.

Introduction

The superior colliculus (SC) of the mammalian midbrain contains topographic representations of visual, auditory, and somatosensory space that are in anatomical spatial register with each other (King, 1999). The alignment of these 'maps' of multi-modal space is thought to enable the animal to orient more effectively to a variety of spatial stimuli, for example, re-orienting its gaze towards a sound emanating from outside of the visual field. The output neurons of the SC contact pre-motor neurons responsible for eye and head-orienting movements (and the ears in some animals), further implicating the SC in the control of gaze and orientation.

The SC is a laminated structure, and represents different modalities within the different cytoarchitectural layers. Layers II to III are primarily visual in nature, while layers IV-VI show auditory, somatosensory, and multi-sensory activity including bi-modal and tri-modal responses (see Figures 1 and 2). Visual projections from the retina and several other areas (visual thalamus and extra-striate cortex) synapse onto neurons in the superficial layers, while auditory projections from the inferior colliculus and other brainstem nuclei converge in the deeper layers. Some early single unit recording studies (Wickelgreen, 1971; Stein *et al*., 1975; Harris *et al*., 1980) found an approximate alignment of visual, auditory and somatosensory receptive fields, as the recording electrode penetrated successively deeper layers. For example, cells with visual receptive fields in the centre of the visual field (0º azimuth and 0º elevation) were aligned with cells having auditory best responses from stimuli from the same location in space, and a somatosensory receptive field on the nose or on the face. Importantly, cells in the intermediate and deep layers were bi-modal or tri-modal, having for example both auditory and visual receptive fields anchored to the same point in space.

Unlike the visual projection, which is roughly topographic from birth and shows spatial selectivity even before eye-opening (probably due to an experience-independent mechanism similar to that which drives the development of the optic tract), auditory projection topography must be computed from a variety of non-spatial signals such as the inter-aural time and level differences of sounds arriving at both ears, which are computed in the adult medial and lateral superior olives, respectively (King *et al*., 2000). It is thought that, in the superior colliculus, visual signals act as a template under which auditory topography is supervised. A major problem for the development of this topography, is that the visual map is represented in eye-centred space (i.e. a retinotopic projection), whereas the auditory map is constructed from head-centred cues (the difference in arrival time and amplitude of sounds arriving at each ear), and the somatotopic

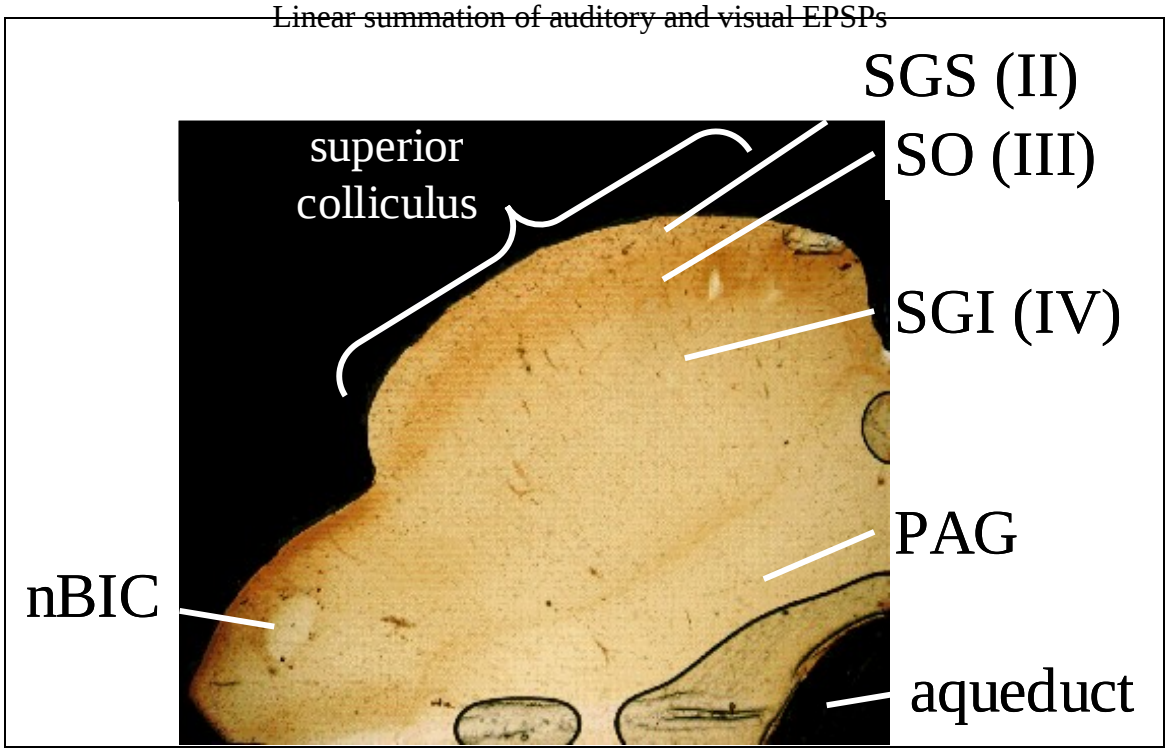

Figure 1. Photomicrograph of a coronal section of the rat midbrain. *Only the left dorsal quadrant of the midbrain section is shown. The laminated structure of the superior colliculus is clear - the different laminae are labelled. Layers II and III are the superficial, 'visual' layers. Layer IV is the intermediate layer where most multi-sensory cells are found. Deeper than layer IV, the SAI and SGP layers also contain multi-sensory cells. The irregular black-outlined shapes are artefacts of the staining and mounting procedure. nBIC - nucleus of the brachium of the inferior colliculus, SGS - stratum griseum superficiale (layer II), SO - stratum opticum (layer III), SGI - stratum griseum intermediale (layer IV), SAI - stratum album intermediale (layer V) SGP - stratum griseum profundum (layer VI), PAG - peri-aqueductal grey*

map represents the whole body. Since the auditory map is a computational one, whereas visual and somatotopic maps are already spatially organised (the retina and the body can be considered two-dimensional receptor ‘sheets’ which project topographically to their SC representation), it is hypothesised that auditory topography is brought about under visual guidance.

Knudsen and Brainard (1991; Knudsen, 1998; Brainard and Knudsen, 1998) studied the visual guidance of auditory topography by placing refracting prisms in front of barn owls’ eyes during development. The prisms displaced the visual field with respect to the head by 23º to the left or the right. Thus, when single visual units in the superficial SC were recorded after extended experience of the displaced visual world, those neurons that used to respond to stimulation from the centre of the field, now responded to stimuli from 23º to the side. When auditory responses were examined in the deeper layers of the SC, they found that the auditory map in the SC had shifted in an adaptive direction, thereby maintaining auditory and visual alignment. This adaptation was limited to a critical period, and was dependent on the amount and quality of environmental and social richness of the animal’s housing. Similarly, both sectioning of an extra-

ocular muscle, which deviates the whole eye by 15-20º; and rotation of the eyeball within its socket (a deviation of up to 180º), led to an adaptive adjustment of auditory spatial tuning of individual neurons. In the first case auditory topography adjusted towards the abnormal visual topography, but in the second the deviation was very disruptive and auditory topography did not develop (King *et al*., 1988; King and Carlile, 1993); the result was a disordered auditory map. Thus, it seems that visual guidance of the auditory topography is limited to a developmental critical period (Brainard and Knudsen, 1998) and by the severity of the visual perturbation (King *et al*., 1988).

King and co-workers (1998) carried out a more direct examination of the influence of descending superficial visual activity in the SC for the refinement of the deep SC auditory map. By introducing small lesions restricted to a portion of the SC and extending only into the superficial layers, it was possible both to examine visual receptive field properties in the spared superficial layers, and auditory receptive fields under the normal and the lesioned layers. The auditory *spatial tuning* of single neurons underneath the lesioned area was only slightly affected by deprivation of the overlying superficial layers. However, auditory *topography* across the lesioned SC was severely disturbed, with many units having auditory receptive field best positions well outside the normal range (as predicted by their distance from the rostro-lateral border of the SC). When similar lesions were made in adult animals, there was no such alteration in auditory topography. Similarly, administration of NMDA-receptor antagonists to the superior colliculus of normal ferrets during development results in abnormal auditory topography similar to that produced by visual perturbations (Schnupp *et al*., 1995; King *et al*., 1998b).

These studies imply that there is a critical period during which patterned, topographic visual input from the superficial layers of the superior colliculus is required in order that a normal, adult-like auditory topography can develop among the acoustically-responsive multi-sensory cells in the deeper layers, and that this experience-dependent plasticity relies on excitatory glutamatergic transmission in the superior colliculus. Despite the key importance of understanding the development of sensory map alignment, little is known about the cellular or molecular basis for the visual guidance of auditory topography in the developing SC (Wallace and Stein, 1997; King, 1999).

The deep layers of the superior colliculus receive their primary auditory projection from the inferior colliculus *via* the nucleus of the brachium of the inferior colliculus (nBIC) (Schnupp and King, 1997), and smaller auditory projections from the external nucleus of the inferior colliculus

(ICX) and other midbrain and cortical areas (King *et al*., 1998a). Cells in the deep layers also receive mono- and poly-synaptic visual projections from the superficial layer visual map (Lee *et al*., 1997). Deep layer cells are thus 'multi-sensory' and are a putative cellular substrate through which visual-auditory topographic alignment is brought about. The synaptic input from superficial visual to deep layer multi-sensory cells might provide sufficient depolarisation in the latter to amplify or strengthen auditory projections that were co-incidentally active. Since the visual projection is topographic from birth, only those active auditory neurons that also synapse onto the multi-sensory cell would be facilitated, while other inputs would remain unchanged or be depressed.

We studied the sub-threshold integration of excitatory visual and auditory signals in the deep layers of the SC, using whole-cell current clamp recordings from *in-vitro* midbrain slice preparations taken from rats before normal eye-opening (postnatal days 11-16). First, we asked whether excitatory post-synaptic potentials (EPSPs) evoked in deep layer multi-sensory cells following stimulation of both the nBIC and the sSC were integrated by linear summation in the cell. Second, we asked whether the temporal offset between nBIC ('auditory') and sSC ('visual') stimulation had any bearing on the synaptic integration of signals from these projections. The temporal offset between auditory and visual stimulation (hetero-synaptic) was compared with paired-pulse stimulation of each modality alone (homo-synaptic). We found that auditory- and visual-evoked EPSPs summed linearly at the soma of deep layer multi-sensory cells, and that these two responses were temporally independent, whereas paired-pulse stimulation led to homo-synaptic facilitation in the deep layer cells.

Methods:

Animals

24 Long-Evans Hooded and 2 Sprague-Dawley rats aged between postnatal day 11 and 16 inclusive were used in the experiments. All experimental procedures and husbandry conditions were approved under licence from the Home Office.

Slice Preparation

For each experiment, a single pup was decapitated, and the scalp, cranium, and cerebral cortex were quickly removed to expose the dorsal surface of the midbrain. A segment between the diencephalon rostrally and the inferior colliculus caudally was dissected out and transferred to ice-cold (0 – 2º C) artificial cerebro-spinal fluid (aCSF) containing (in mM) 124 NaCl, 26 $NaHCO_3$, 2.3 KCl, 1.26 KH_2PO_4, 1.0 MgS_4-$7H_2O$, 10 Glucose, 2.5 Calcium, at an osmolarity of 315-320 mOsm. All solutions were bubbled with 95 % oxygen and 5 % CO_2 (carbogen). After cooling for 10 minutes, the brainstem segment was mounted on a Vibratome slice cutter. Two or three 500 µm coronal slices through both the superior colliculus and the brachium of the inferior colliculus were obtained from each animal. The slices were transferred to a chamber containing aCSF at room temperature, and bubbled continuously with carbogen until use in the recording chamber.

Slice Mounting and Microscopy

Slices were mounted in dishes under an Axioskop microscope (Zeiss, Germany), with differential interference contrast infra-red enhancement, displayed on a monitor. Slices were bathed in aCSF flowing continuously at approximately 100 ml/hr and bubbled with carbogen. In the first seven experiments presented here, the aCSF was maintained at room temperature (23 – 24º C), in the last three experiments, aCSF was maintained at 29 – 30º C by heating the aCSF prior to bath application. Bath temperature was monitored electronically, and the heating element adjusted manually. During recording, 4 µM bicuculline (a competitive $GABA_A$ antagonist) was applied to the bathing solution to block inhibitory synaptic activity.

Electrodes

Two strands of Teflon-coated silver wire twisted around each other served as the nBIC-stimulating electrode. The superficial layer-stimulating electrode was pulled in two stages from a double-barrelled (‘theta’) borosilicate glass capillary tube of 2 mm diameter, with a silver/Teflon-coated wire electrode inserted in each barrel. The final tip diameter was 1-3 µm.

The barrels were filled with aCSF. The patch recording microelectrodes were pulled in two stages from a borosilicate glass capillary (1.5 mm outer and 1.17 mm inner diameter), to form a tip of 3 – 4 µm diameter. Patch electrode input resistance was 5-10 mega ohms. Recording micropipettes were filled with (in mM) 130 potassium gluconate, 20 HEPES, 6 KCl, 3 NaCl, 2 Mg-ATP, 0.5 EGTA, 0.3 GTP-Na, and 0.5 % biocytin, with osmolarity at 289 mOsm. The recording electrode and a separate reference bath electrode were chloride-coated prior to each experiment.

Whole-Cell Patch Recording

An Axoclamp 2B amplifier was interfaced with two constant voltage or constant current stimulators, and TTL-pulse controllers. The hardware was controlled using Axograph software on an Apple Macintosh personal computer. Current-clamp recordings were obtained in the 'bridge' mode of the amplifier.

Suitable cells were identified morphologically in the intermediate/deep layers of the superior colliculus (the *stratum griseum intermediale*, SGI, layer IV). Typically, recorded cells were large and their somata were round, ovate, or pyramidal in shape, having one or two prominent dendrites. Positive pressure (approximately 150 mBar) was applied to the recording electrode, such that an effluence of electrode solution was visible under the microscope. The electrode was positioned over the target cell, and slowly lowered under visual guidance to within a few micrometers of the cell body, such that the flowing electrode solution 'dimpled' the cell membrane. At this point, positive pressure was abruptly released, and negative pressure was slowly increased, sucking the cell membrane into a tight, giga-ohm resistance seal with the patch electrode. Further increases in negative pressure, either slowly or in abrupt steps, or *via* the application of a brief voltage pulse to the membrane, broke through the membrane, forming a continuous channel between the pipette and intra-cellular solution. This produced an abrupt decrease in recorded membrane potential to between –50 and –80 mV, and the presence of several clear, sharp spikes. The electrode pressure was released, and a series of increasing voltage deflections was applied through the recording electrode to check for the presence of clear, sharp action potentials. This was repeated during the experiment; resting and spike-threshold potentials, the amplitude and width of induced spikes, spontaneous activity and the holding current were monitored regularly. Typically, a small negative current (-50 ± 20 pA) was injected to hyperpolarise the cell to between –70 and –60 mV. Five cells were held sufficiently long for data at several different membrane resting potentials to be obtained. In these situations, holding current was increased or decreased to depolarise or hyperpolarise the membrane

potential to approximately 10 mV from the initial level (i.e. to between –60 and –50 mV or between –80 and –70 mV respectively).

Stimulation

The nBIC electrode was lowered into a position slightly medial to the surface of the BIC, and rested on the slice. The sSC electrode was lowered onto the superficial layers of the SC (between *stratum griseum superficiale* (SGS, layer II) and *stratum opticum* (SO, layer III)), in an approximately radial columnar position (Lee *et al*., 1997; Skaliora *et al*., 2002), relative to the patched cell. See Figure 2.

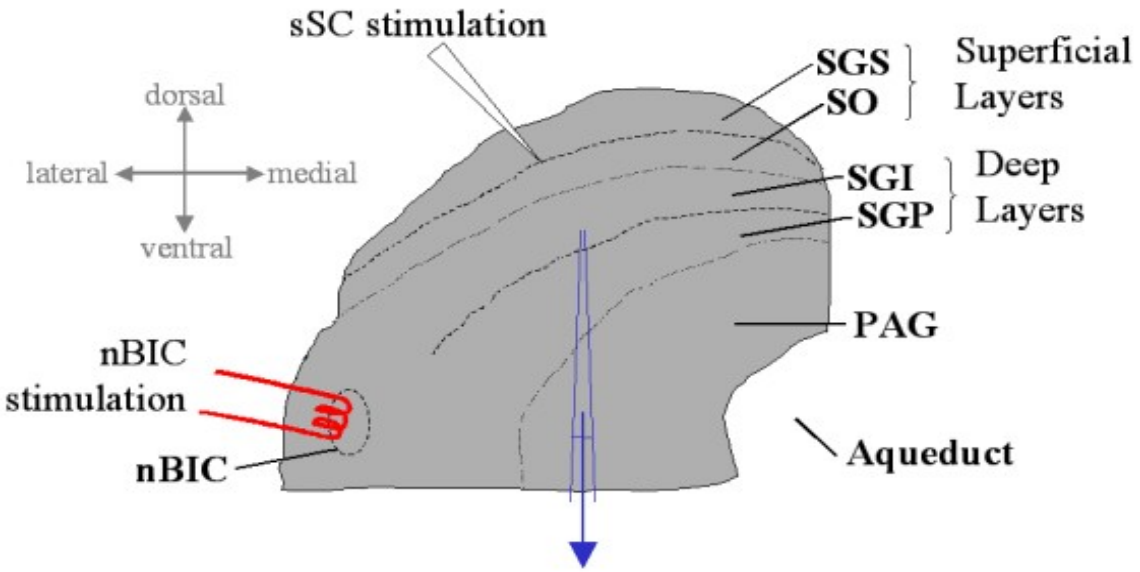

Figure 2. Superior colliculus stimulation and recording procedure*. The coronal midbrain slice was mounted whole under a microscope, only one quadrant of the slice is shown here for clarity. The broken lines represent the boundaries between the major layers of the SC. Several layers (SZ, SAI and SAP) are not shown for clarity. Cells were identified in the deep layers, and patched with a glass microelectrode (blue). Stimuli were delivered to the superficial layers (sSC) via another glass microelectrode (white), and to the nucleus of the brachium of the inferior colliculus (nBIC) through a twisted silver wire (red). Abbreviations as in Figure 1*

A constant voltage (first five experiments) or constant current (last five experiments) pulse (0.2 ms duration, amplitude specific to each cell – see results) was applied to each stimulation electrode in turn while recording from the patched cell. The stimulation intensity was increased until reliable monosynaptic responses (defined as having a latency variability of two milliseconds or less) were recorded. If no such responses were found at the stimulator's maximum intensity, either the stimulation electrodes were moved to an alternative location, or a different cell was patched. Valid recordings were those where both nBIC and sSC responses in

the patched cell were monosynaptic, and at least the first 20 ms of the EPSP evoked was not normally 'contaminated' with secondary or tertiary (poly-synaptic) events. This was to ensure that the measured EPSP summation at the soma of recorded cells was due only to single, monosynaptic EPSPs, and not subsequent events arising from different pathways or interconnections – this allowed firmer conclusions about post-synaptic integration to be drawn.

Several stimulation protocols were run, for each cell at each membrane potential. In all cases, 25 repetitions were carried out, at an inter-trial interval of 5 seconds. The stimulation intensity was held constant for each cell and membrane-potential studied:

Protocols:

Linear summation – nBIC and sSC stimuli were timed to ensure the EPSPs evoked in the recorded cell began coincidentally. In practise, a 5 msec offset between nBIC (first) and sSC (second) stimuli was sufficient for this purpose, since nBIC latencies are usually between 9 and 12 msec, and sSC latencies between 4 and 7 msec.

Temporal independence – nBIC and sSC stimuli were separated by 50 msec. Typically, the second EPSP was superimposed on the tail of the first, since EPSP decay was not complete by this stage. Both nBIC followed by sSC, and sSC followed by nBIC stimulations were performed. Further, paired-pulse stimulation of the same projections was carried out to assess homo-synaptic effects: both nBIC and sSC were stimulated twice separately, at an interval of 50 msec. During these protocols, responses to single stimuli were recorded again for comparison.

Timecourse – For two cells, temporal independence was assessed at a range of additional time points, the sSC-nBIC offset being ±150, ±100, ±25, and ±15 msec.

For a pictorial representation of the stimulation protocols, see Figure 3.

Analysis

For cells that displayed monosynaptic responses following stimulation of both nBIC and sSC, the amplitude of the initial peak, and the integral of the first 20 msec of the EPSP were measured using Axograph software. All measurements were based on the averaged traces of all trials uncontaminated by large voltage fluctuations or spikes. Measurements were taken from the baseline average resting potential in the 1-5 msec after the stimulus artefact had decayed (and before EPSP onset). The EPSP start time and the peak were discerned manually using the

software. *For the temporal independence protocols, the first EPSP of the two pulses (either hetero- or homo-synaptic was removed from the trace to allow calculation of the second EPSP amplitude. Using the Axograph software, the EPSP to be removed was aligned with the EPSP trace obtained from a single-stimulation protocol, and the latter was then subtracted from the former. This normally resulted in a smooth, flat baseline prior to the second EPSP of interest. On some occasions a small negative or positive peak remained, due to natural variability in EPSP amplitude across trials.* The remaining, single EPSP was then normalised to the baseline resting potential in the 1-5 ms following the stimulus artefact, and measured as above.

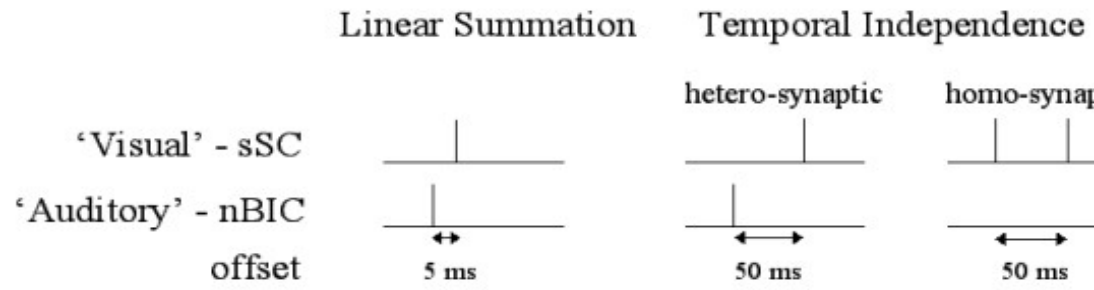

Fi *ulated se msec be . For te nBIC sti poral in perior co*

Most EPSP data are expressed as amplitudes relative to the control, single-stimulation protocol. Data are calculated as percentage values individually for each cell, then averaged over the group. In all cases, paired, two-tailed t-tests were performed on the pair-wise raw amplitude data (in millivolts), since it was the within-cell facilitation or depression of EPSP amplitudes contingent on simultaneous or prior stimulation that we was the crucial test of multi-sensory interaction.. Percentage linearity and temporal independence were calculated as follows;

Linear summation:

$(EPSP_{nBIC+sSC}) / (EPSP_{nBIC} + EPSP_{sSC}) * 100\ \%$

Temporal independence and Timecourse:

sSC hetero-synaptic stimulation: $(EPSP_{nBIC \Rightarrow sSC}) / (EPSP_{sSC}) * 100\ \%$

sSC homo-synaptic stimulation: $(EPSP_{sSC \Rightarrow sSC}) / (EPSP_{sSC}) * 100\ \%$

nBIC hetero-synaptic stimulation: $(EPSP_{sSC \Rightarrow nBIC}) / (EPSP_{nBIC}) * 100\ \%$

nBIC homo-synaptic stimulation: $(EPSP_{nBIC \Rightarrow nBIC}) / (EPSP_{nBIC}) * 100\ \%$

Where,

$EPSP_{nBIC+sSC}$ = nBIC & sSC EPSPs occur simultaneously

$EPSP_{sSC}$ = sSC EPSP occurs alone

$EPSP_{nBIC \Rightarrow sSC}$ = sSC EPSP preceded by nBIC EPSP

$EPSP_{nBIC}$ = nBIC EPSP occurs alone
$EPSP_{sSC \Rightarrow nBIC}$ = nBIC EPSP preceded by sSC EPSP

Histology

Following successful experiments, slices were fixed in 4 % paraformaldehyde and stored at 4º C. The following staining procedures were carried out between 1 and 12 weeks later: Slices were transferred to a 30 % sucrose solution for 3 hours, frozen for ten minutes and thawed at room temperature, then refrozen and re-thawed. The slices were washed three times in phosphate buffer (0.1 M, pH = 7.2) then transferred to plates with 2 ml phosphate buffer containing Triton detergent, 10 µl avidin and 10 µl biotin (left for one hour to complex prior to application to the slices) and lightly agitated overnight at room temperature.

The detergent and avidin-biotin complex (ABC Elite, Vector Labs Peterborough) were washed (4 x 10 minutes) in phosphate buffer under light agitation, then 1 ml of 0.5 mg/ml diaminobenzidine (DAB, Sigma, Poole) in phosphate buffer with 3 x 10^{-5} % hydrogen peroxide was added to each slice, and agitated for ten minutes. The DAB was washed off three times for ten minutes with phosphate buffer, the slices were cleared in methyl salicyclate overnight, and finally mounted in gelatine on microscope slides.

Results

Unless otherwise indicated, all data are expressed as the mean ± the standard error of the mean, and are given to two decimal places. Each data point in the figures represents a cell at a given membrane potential and holding current. Some cells thus contributed two or three data points. All example traces shown in the figures below were selected as representative examples of the recordings, based on their having the median value in the relevant range of data. This results in both some 'clean' and 'noisy' data. In all cases, however, the initial monosynaptic EPSP peak amplitude was always discernible.

Yield of Cells

Twenty-four experiments were carried out over three months, using 26 rats. A total of 108 cells were successfully patched, and these cells were held for between five minutes and three hours. Sixty-six cells were held long enough to assess the response to both nBIC and sSC stimulation. After rejecting cells that did not show clear monosynaptic responses from both nBIC and sSC stimuli, only 20 cells out of 66 (30 %) were subjected to the full experimental protocols. The data from ten of these cells were also rejected during analysis based on the range of latencies for either or both sSC and nBIC EPSP responses (accepted range criterion was $\leq$ 2 msec), and the number of stimuli failing to evoke EPSPs (accepted criterion was < 5 failures). The remaining data for ten cells are presented here. This yield of cells is lower than in previous work in our lab (Skaliora *et al*., 2002), perhaps because it was more important to ensure only monosynaptic inputs in the current study. Two of these cells were recorded at two different membrane potentials (increased/decreased holding current as described in methods), and one further cell was recorded at three membrane potentials. Two cells were only held long enough to perform the linear summation protocol. The last two cells recorded were subjected to all three protocols: linear summation, temporal independence, and timecourse.

Six cells were recovered histologically and examined microscopically. In all cases, the cells were located in layers IV and V, the majority being in the upper- and intermediate-regions of layer IV. The cell bodies were generally round or polygonal in shape, and between two and four prominent dendrites were clearly visible. The dendrites often extended up into layer III, and in several cases, an axon was visible forming a trajectory towards the peri-aqueductal grey layer. At least two types of cell, based on their dendritic morphology were visible in our small sample. Some displayed a columnar (superficial to deep) organisation, while others sent several dendritic branches medially and laterally. Some, like the example in Figure 4 displayed both. It may be

important for future work to correlate cell type with auditory-visual synaptic integration, since a different sub-population of deep cells may exclusively form multi-modal responses. This is discussed further below.

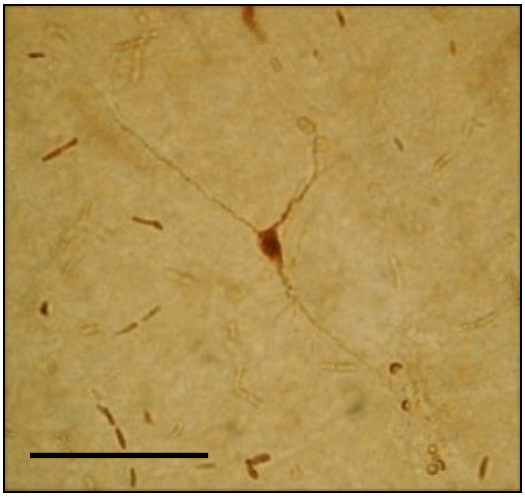

Figure 4. Photomicrograph of a single neuron from layer IV (SGS) of the superior colliculus*. This cell was typical of those in the present study for having two or three prominent dendrites, and a reasonably large cell body. The two dendrites projecting from opposite poles of the cell body are within a columnar organisation, while the large dendrite on the right projects towards the midline. Six (of ten) cells were recovered through the staining procedure, and identified as large cells in layers IV to VI. Scale bar is 100 µm*

Response to Stimulation of the Superficial Layers of the Superior Colliculus

The sSC stimulation intensity used to evoke reliable monosynaptic EPSPs in the patched cell was, for the first five cells 48.80 ± 9.12 V. For the last five cells (and nine data points), the intensity was 3.83 ± 2.89 mA. The EPSP latency for 10 cells (14 data points) following sSC stimulation was 4.55 ± 0.72 msec. Figure 5 (upper right panel) shows a typical cell's response latency following sSC stimulation. The range of latencies reported here is lower than in previous work. Skaliora et al (unpublished) found mean latency of superficial layer to deep layer conduction of 6.4 ± 0.33 msec. The primary contribution to latency is the synaptic delay from the superficial onto the deep cell. Otherwise, latency should vary linearly with distance from the stimulation site, ignoring differences in current spread through the slice. Thus, in the present study it is likely that, on average, cells in the upper layers of layer IV were recorded more frequently, leading to decreased latency. From the histologically recovered cells, three of six were in the upper layers, and only one or two were found below layer V. Of the 350 responses recorded to superficial stimulation (14 x 25 repetitions), only nine were rejected due to action potential contamination or large voltage deflections.

The mean monosynaptic EPSP amplitude evoked by stimulation of the sSC was 1.00 ± 0.12 mV for ten cells (14 data points). The mean integral over the first 20 msec of these EPSPs was 14.89 ± 1.53 mV.ms. Since EPSP amplitude and integral were highly correlated ($r = 0.97$, $p < 0.005$), all further data analyses will deal only with the monosynaptic peak amplitude. Figure 5 (left

panel) plots example EPSP traces from one cell, plots the latency variability of responses in this cell (upper right panel), and also shows the relationship between EPSP amplitude and integral (lower left panel), which serves to illustrate the range of EPSP amplitudes and integrals. The regression of the EPSP integral (y) on EPSP amplitude (x) yielded y = 11.95x + 2.92. The positive intercept on this regression probably reflects the presence of additional EPSPs under the 20ms integral, which did not otherwise affect the initial peak amplitude. It is therefore also safer to use the amplitude as our measure of EPSP size.

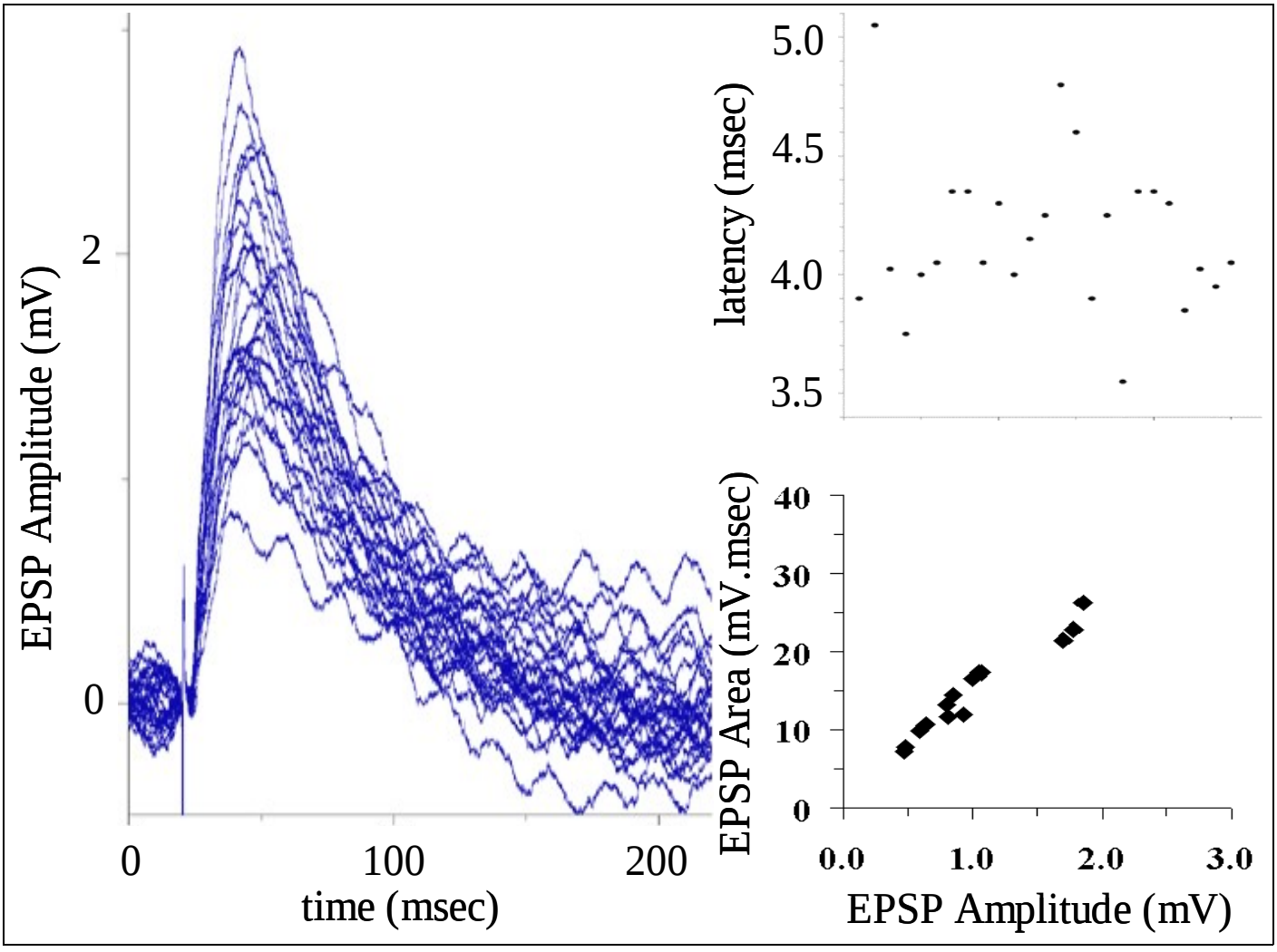

Figure 5. Response to superficial superior collicular stimulation. ***Left Panel****: 25 EPSPs aligned in the vertical direction in the 1-3 msec before the start of the EPSP. The range of EPSP amplitudes (0.8 to 2.9 mV) shows the large inter-EPSP variation. The oscillatory component in the traces is contamination from electrical noise.* ***Upper Right Panel****: Distribution of EPSP latencies for the same cell as shown in the left panel.. Cells having a latency range of >2 msec were rejected. The range in this example is 1.6 msec.* ***Lower Right Panel****: Relationship between EPSP amplitude (x-axis) and EPSP integral (y-axis) measured over the first 20 msec of the EPSP*

Response to Stimulation of the Nucleus of the Brachium of the Inferior Colliculus

The nBIC stimulation intensity used to evoke reliable monosynaptic EPSPs in the patched cell was, for the first five cells 63.90 ± 11.53 V. For the last five cells (and nine data points), the intensity was 26.99 ± 12.87 mA (see Figure 6, left panel, for typical EPSPs evoked by nBIC stimulation.

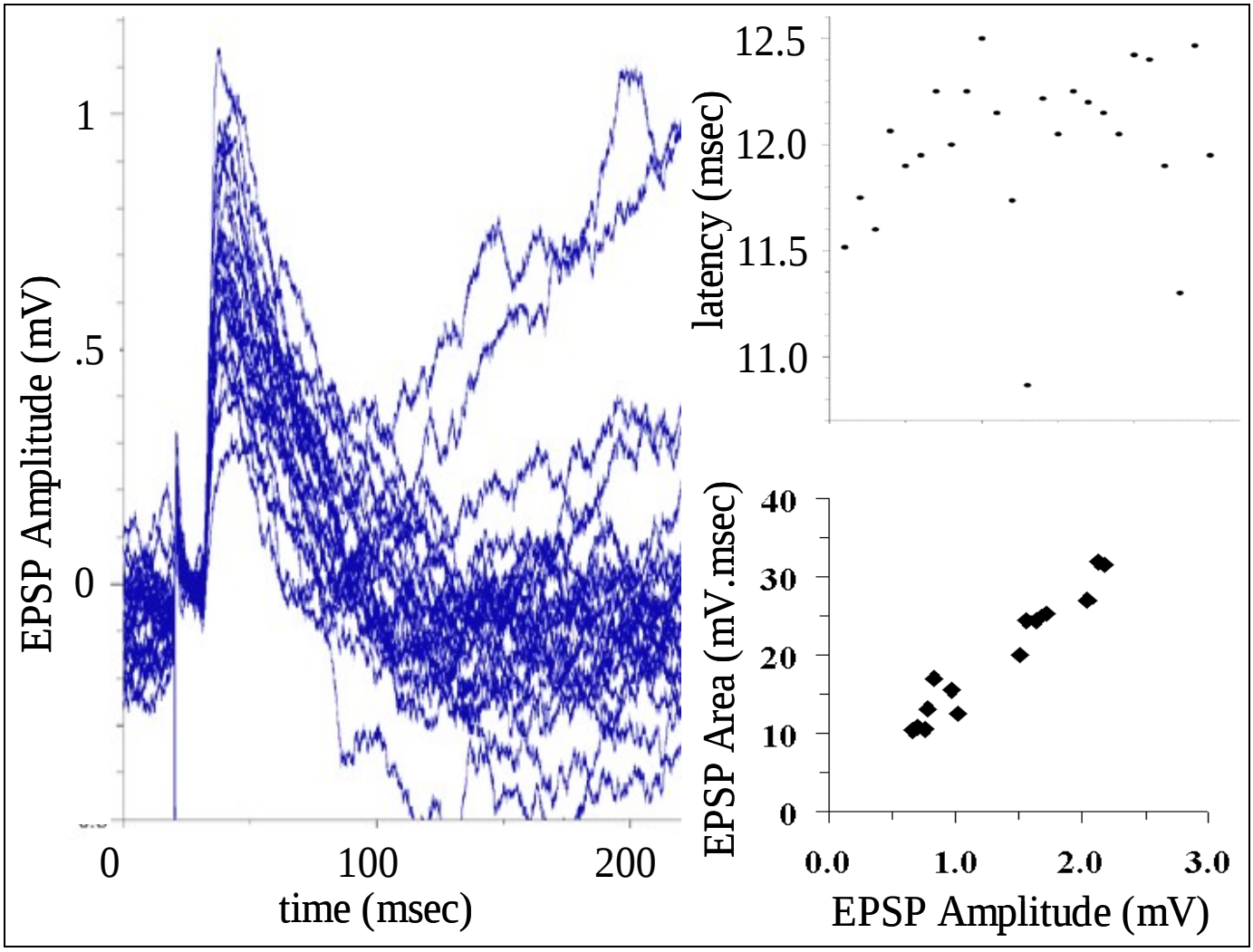

Figure 6. Response to stimulation of the nucleus of the brachium of the inferior colliculus. ***Left Panel****: 25 EPSPs aligned in the vertical direction in the 3-5 msec before the start of the EPSP. The range of EPSP amplitudes (0.8 to 2.9 mV) shows the large inter-EPSP variation. The oscillatory component in the traces is contamination from electrical noise.* ***Upper Right Panel****: Distribution of EPSP latencies for the same cell as shown in the left panel.. Cells having a latency range of >2 msec were rejected. The range in this example is 1.6 msec.* ***Lower Right Panel****: Relationship between EPSP amplitude (x-axis) and EPSP integral (y-axis) measured over the first 20 msec of the EPSP.*

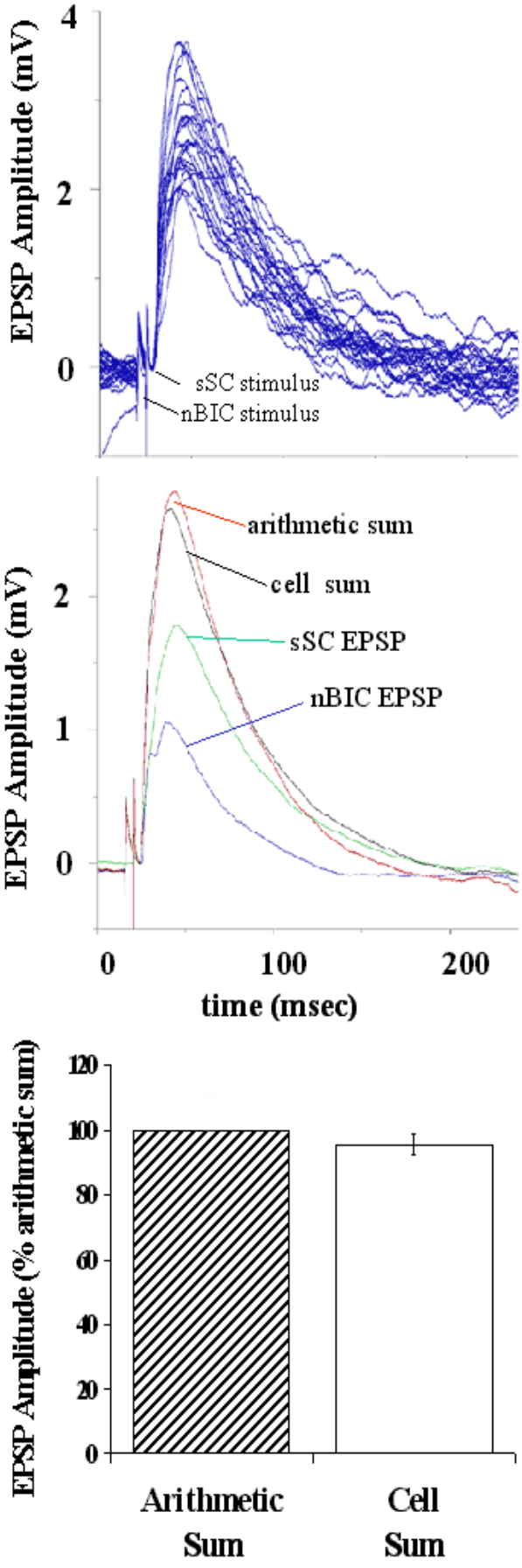

Figure 7. Summation of coincident EPSPs. Upper Panel*: Representative example of 25 EPSPs following dual nBIC and sSC stimulation. The stimulus artefacts are visible as sharp deflections approximately 10 and 5 msec before EPSP onset respectively.* ***Middle Panel****: The data from the upper panel (cell sum, black trace) were averaged and plot against individual nBIC- (blue) and sSC-evoked (green) EPSP responses, and the arithmetic sum of these EPSPs (red). The example shown displays a slightly sub-linear summation.* ***Lower Panel****: Average coincident EPSP summation (cell sum) of 10 cells (14 data points) compared to the arithmetic sum. The slight sub-linearity overall is not significantly different from linearity (100 %)*

The EPSP latency for 10 cells (14 data points) following nBIC stimulation was 10.68 ± 0.87 msec. Figure 6 (upper right panel) shows a typical cell's response latency following nBIC stimulation. Previous work in our lab found an average response latency following nBIC stimulation of 12.04 ± 0.92. This difference may be due to cells in the present study being on average more laterally positioned than in the previous studies, although a general decrease in latencies for other reasons (such as increased myelination in the brain slices used here) can not be ruled out. One response (out of 350) was rejected due to action potential contamination or large voltage deflections.

The mean monosynaptic EPSP amplitude evoked by stimulation of the nBIC was 1.32 ± 0.15 mV for ten cells (14 data points). The mean integral over the first 20 msec of these EPSPs was 19.56 ± 2.08 mV.ms. EPSP amplitude and integral were highly correlated with eachother ($r = 0.97$, $p < 0.005$). See Figure 6 (lower right panel) for the range of EPSP amplitudes and integrals. The regression of EPSP integral (y) on EPSP amplitude (x) yielded $y = 13.39x + 1.90$. For the same reasons as given for the sSC data above, all further analysis deals only with EPSP amplitude.

Linear Summation

The amplitude of EPSPs evoked in the patched cell from coincident stimulation of nBIC and sSC projections was 2.14 ± 0.18 mV. This equates to 95.33 ± 3.32 % of the arithmetic sum (2.27 ± 0.19 mV). This difference (absolute values) was not significant (2-talied, paired t-test, $p = 0.10$). Figure 7 plots this result, along with example traces of the dual-stimulation evoked EPSPs, and the average single, arithmetic, and dual traces of a representative example.

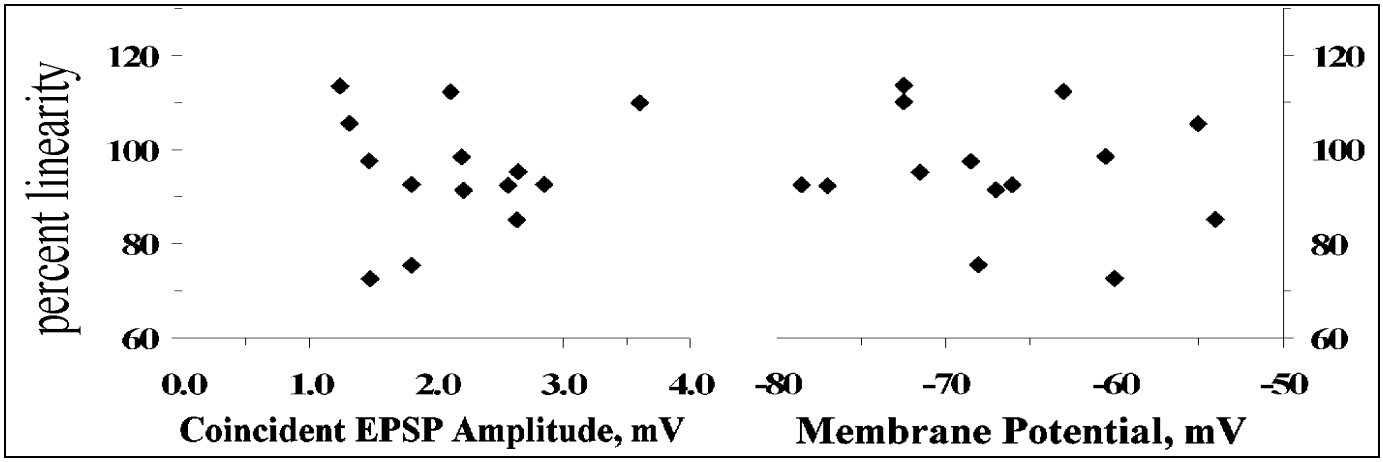

Figure 8. Relationship between EPSP summation, EPSP amplitude and membrane potential. Left Panel*: Linearity of EPSP summation (percent linearity, y-axis) against the coincident EPSP amplitude. The graph shows that EPSP summation is independent of EPSP amplitude.* ***Right Panel****: The same data plot against membrane potential. EPSP summation is also independent of the cell's resting membrane potential*

EPSP summation may become non-linear at different membrane potentials or for different sized EPSPs (see discussion, below). These phenomena may be due to the activation of voltage-sensitive cation channels, boosting EPSP summation, or changes in the driving force for the EPSP (i.e. sodium channels are closer to their reversal potentials at more positive membrane potentials). Figure 8 shows the ratio of coincident EPSP summation by the cell to that of the arithmetic sum (percent linearity), plotted against the membrane potential at which the

recordings were made (left panel) and the combined amplitude of the co-incident EPSP (right panel). Neither membrane potential ($r = -0.15$, $p > 0.1$) nor EPSP amplitude ($r = 0.08$, $p > 0.10$) correlated significantly with the ratio of coincident : arithmetic summation. This suggests either that no active membrane currents were contributing to the observed linear summation, or that there was a balance of inward and outward active currents.

Temporal Independence

Responses evoked by sSC stimulation alone (EPSP amplitude = 0.77 ± 0.14 mV) were not significantly different (2-tailed, paired t-test, $p = 0.87$) from sSC-evoked EPSPs preceded 50 msec earlier by an nBIC-evoked EPSP (sSC EPSP amplitude = 0.78 ± 0.11 mV or 112.88 ± 11.2 % of the response to single stimulation). The value for EPSP amplitude here (0.77 ± 0.14 mV) is different in this case from that presented for the same stimulus earlier (1.00 ± 0.12 mV), since the single stimulation protocol was repeated to reduce the effects of time and membrane potential drift on the data. This difference was not significant (2-tailed, paired t-test $p = 0.14$), indicating that the two samples were representative of the same population of responses. For the paired-pulse, homo-synaptic stimulation protocol, the difference between the second sSC-evoked EPSP (amplitude = 1.24 ± 0.27 mV, or 144.36 ± 14.47 %) and the first (amplitude = 0.77 ± 0.14 mV) was significant (2-tailed, paired t-test, $p = 0.036$). Figure 9 displays these data graphically with a representative example trace for each protocol.

For nBIC stimulation-evoked EPSPs, the difference between single nBIC-evoked EPSPs (amplitude = 1.21 ± 0.16 mV) and nBIC-evoked EPSPs preceded 50 msec earlier by a sSC-evoked EPSP (nBIC EPSP amplitude = 1.27 ± 0.16 mV, or 107.78 ± 6.10 % of the response to a single stimulus) was not significant (2-tailed, paired t-test, $p = 0.32$). Again, different samples of responses to single nBIC stimulations were taken, and this sample did not differ significantly from the sample mentioned earlier ($p = 0.62$). For paired-pulse homo-synaptic stimulation, the second nBIC-evoked EPSP (amplitude = 2.23 ± 0.32 mV, or 178.67 ± 13.85 %) was significantly larger (2-tailed, paired t-test, $p = 0.0004$) than the first nBIC-evoked EPSP 50 msec earlier (amplitude = 1.24 ± 0.16 mV). Figure 10 shows these results alongside representative example traces

There were no significant correlations ($p > 0.05$, not shown) between the temporal independence data and both the membrane potential at which the responses were measured, and the amplitudes of the first or second EPSPs. This would seemingly rule out any post-synaptic voltage-dependent mechanisms for the independence of hetero-synaptic integration and homo-synaptic facilitation.

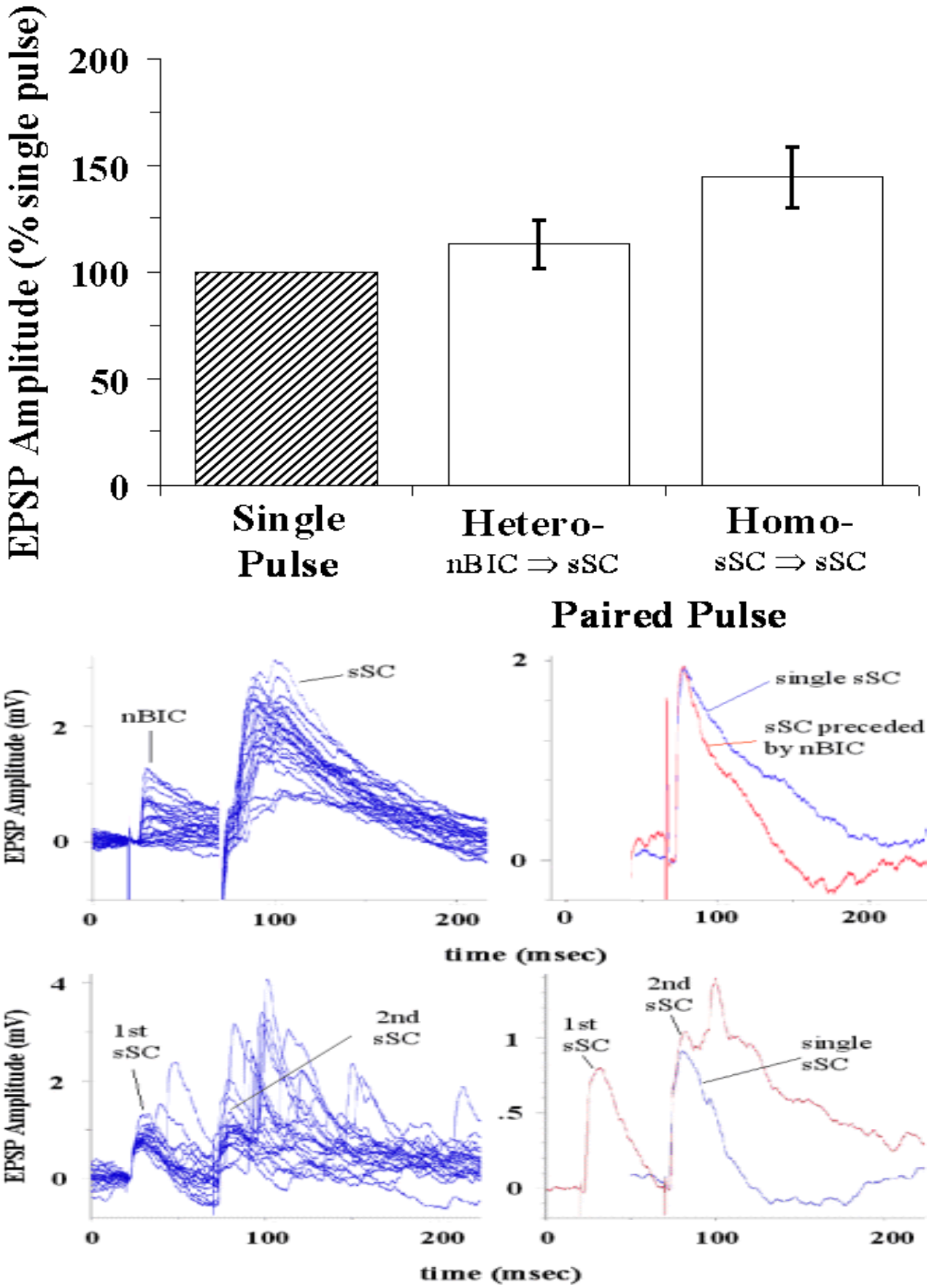

Figure 9. Temporal independence of sSC-evoked responses. Upper Panel*: Relative amplitudes of EPSPs evoked by (from left) single sSC stimulation, sSC stimulation preceded by nBIC stimulation (Hetero-), and sSC stimulation preceded by sSC stimulation (Homo-). Neither hetero- nor homo-synaptic protocols produced a significant change in EPSP amplitude.* ***Lower Panels****: Example traces for hetero- (upper) and homo-synaptic (lower) protocols. 25 traces are shown for each protocol separately on the left, and averaged alongside the comparison single sSC averaged EPSP trace*

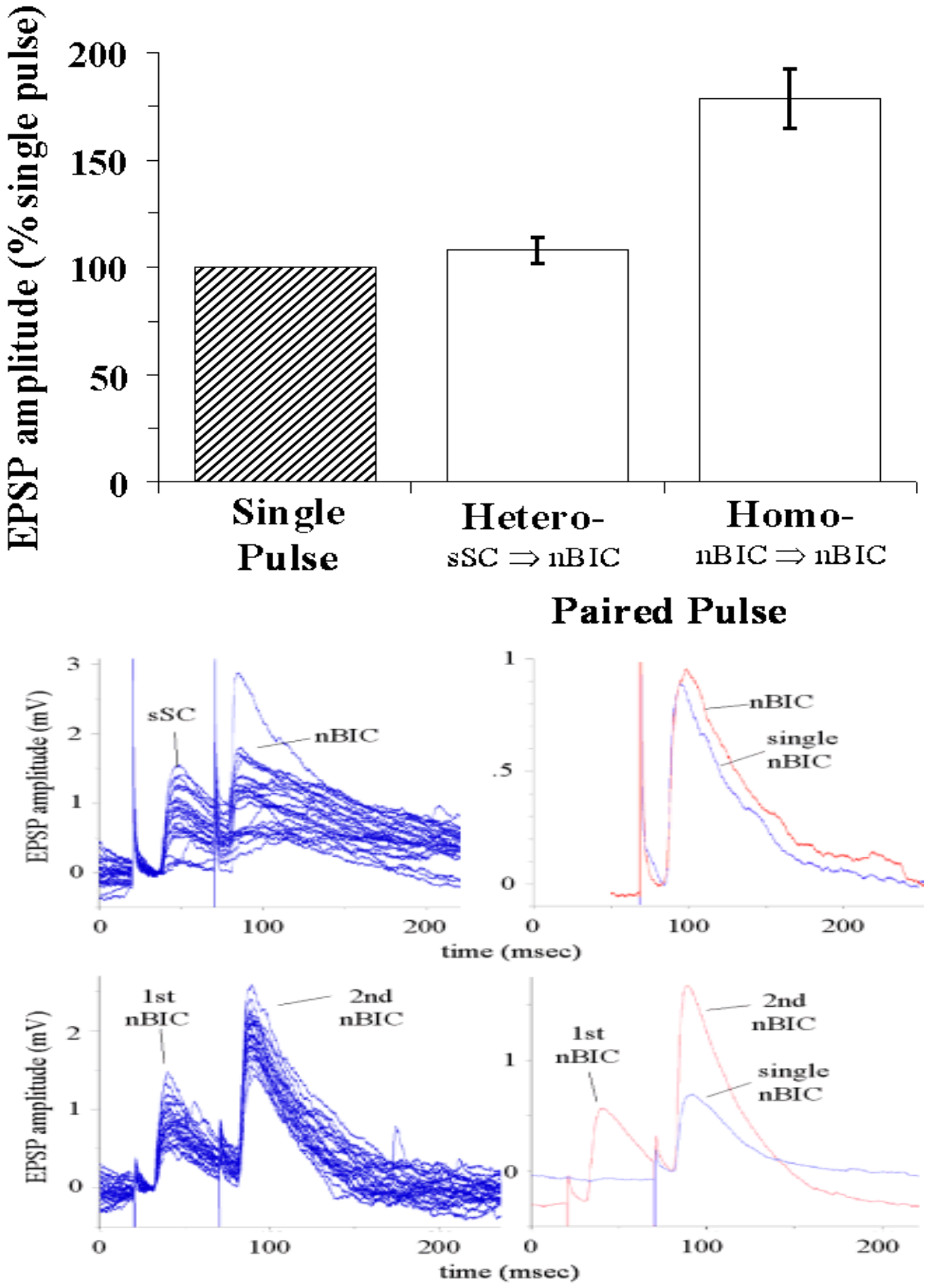

Figure 10. Temporal independence of nBIC-evoked responses. ***Upper Panel****: Relative amplitudes of EPSPs evoked by (from left) single nBIC stimulation, nBIC stimulation preceded by sSC stimulation (Hetero-), and nBIC stimulation preceded by nBIC stimulation (Homo-). Homo-synaptic stimulation produced a significant facilitation of EPSP amplitude.* ***Lower Panels****: Example traces for hetero- (upper) and homo-synaptic (lower) protocols. 25 traces are shown for each protocol separately on the left, and averaged alongside the comparison single sSC averaged EPSP trace.*

Timecourse

Two cells were subjected to the time-course protocol, with varying onset asynchrony between nBIC and sSC stimulation. The first cell was recorded at two resting potentials (varying between –62 and –59.5 mV, and between –74.5 and –70 mV). The second cell was recorded at between –70.5 and –62 mV. Figure 11 displays these data. Each graph displays the data for one cell at one membrane potential, and n = 1 for all the data points except 'indep' which displays the mean and standard error for the pooled data presented above under 'Temporal Independence'. With such few data points, all that can be said is that all the points lie within or just outside the range of values for the temporal independence tested with a 50 msec onset asynchrony. However, the first cell at low membrane potential (-62 to –59.5) shows a large hetero-synaptic *facilitation* when nBIC preceded sSC by 150 msec, and a large hetero-synaptic *depression* when sSC preceded nBIC by 15 to 150 msec. Five of the six data points for this cell are just outside the range of all the data for the 14 cells presented above, measured at inter-stimulus intervals of 50 msec. The two other traces in Figure 11 lie well within the normal range of data (shown by the broken lines) except for one point at –15 msec. This may be a measurement inaccuracy, since the EPSPs from the two stimuli were very hard to separate at this time-point due to their relative latencies. This same caveat applies for –25, and +15 msec time-points.

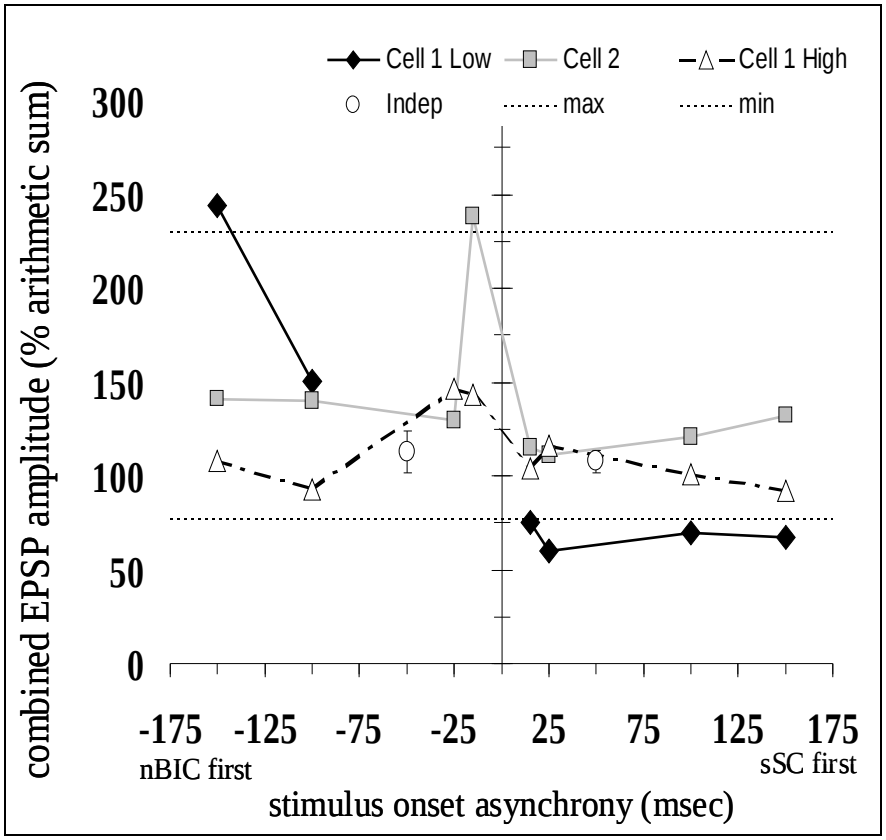

Figure 11. Timecourse of nBIC-sSC sub-threshold interactions*. The nBIC and sSC projections of two cells were stimulation at a range of temporal onset asynchronies (x-axis). The ratio of the second EPSP to the first EPSP (y-axis) indicates temporal independence within the normal range for most data points. Cell 1 (solid diamonds and black lines, open triangles and broken lines) was held at two different membrane potentials (low and high - see text for details). Cell 2 (grey squares and grey lines) was held at one membrane potential. The broken horizontal upper and lower lines show the maximum and minimum of all cells at 50 msec temporal offset. The mean of this data is displayed as two single data points (indep, open circles)*

Discussion

This original research explored two important aspects of auditory-visual sub-threshold interactions in the rat superior colliculus. Firstly, we set out to examine the sub-threshold integration of auditory and visual signals in the deep-layer multi-sensory cells of the rat superior colliculus. We found that, for cells that received monosynaptic projections from both the nucleus of the brachium of the inferior colliculus (nBIC) and the superficial layers of the superior colliculus (sSC), excitatory post-synaptic potential (EPSP) summation, as measured at the soma, was linear. That is, the amplitude of the EPSP resulting from co-incident stimulation of these two pathways was reliably predicted by, and not significantly different from, the arithmetic sum of the EPSP amplitudes evoked by single stimulations.

Secondly, we studied the temporal independence of EPSPs evoked by stimulating the two pathways. We found that EPSP amplitude following sSC-stimulation was unaffected by nBIC-evoked EPSPs 50 msec before, and that nBIC-stimulation evoked EPSPs were unaffected by sSC-evoked responses 50 msec before. In contrast, for paired-pulse, homo-synaptic stimulation, a highly significant facilitation was recorded for responses evoked by nBIC stimulation, such that the second EPSP amplitude was, on average, 78 % larger than the first EPSP occurring 50 msec earlier. A similar effect was seen for sSC-stimulation evoked responses (44 % facilitation of the second EPSP amplitude), but at a lower significance level. Finally, varying the temporal offset between nBIC and sSC stimulation had no discernable *systematic* effects in the two cells that were studied in this protocol. One cell did show several responses outside the range of all other data thus far recorded, and the cell showed a large facilitation for sSC stimuli preceded by nBIC stimuli, and a large depression for the reverse case. These latter data are preliminary, however, and no firm conclusions can be drawn concerning the precise temporal relationship between nBIC and sSC activity and their summation at the soma of deep layer multi-sensory cells, however, if individual cells do show very specific temporal windows within which supra-linear integration of EPSPs or EPSP amplification will occur, then clearly this is of importance for the present study, and further work should address this.

Linear Summation of Sub-threshold Events

Several recent studies have reported linear summation of post-synaptic potentials, for example EPSPs and IPSPs sum linearly in cat visual cortex simple cells (Ferster and Jagadeesh, 1992). In the rat hippocampus, summation was linear in both primary neuronal cell cultures (Cash and Yuste, 1998), and in *in-vitro* brain slices (Cash and Yuste, 1999). However, sub-linear

summation was also found, which depended on the precise position on the dendritic tree that stimulation was applied (Cash and Yuste, 1999). When two stimuli were iontophoretically directed to the apical dendrite, or to the apical and an oblique dendrite, EPSP summation as measured at the soma was sub-linear. In all other stimulus combinations (on basal, apical, and oblique dendrites), summation was linear. Larkum and colleagues (1998) studied motoneurons in rat spinal cord, a preparation similar to that of the present study, and also found linear summation of EPSPs distributed throughout the dendritic tree. There may be species differences in linear summation, however, since spinal cord motoneurons in the tadpole *Xenopus*, integrated EPSPs non-linearly (Wolf *et al*., 1998). In a study similar in many respects to the present one, Nettleton and Spain (2000) found linear and supra-linear summation in pyramidal neurons of rat neocortex. In those neurons that displayed supra-linear summation, an active, regenerative process was apparent. This excitatory component was activated in the first few milliseconds of the EPSP, and was not observed when stimuli were separated in time greater than 10 msec.

Summation of post-synaptic potentials is often interpreted according to the passive, 'cable' model of dendrites. This holds that two stimuli causing post-synaptic potentials will interact to result in sub-linear summation if they are sufficiently close to each other, typically on the same dendritic branch (e.g. Tamás *et al*., 2002). Sub-linear summation follows either from the decreased driving force for subsequent or coincident depolarisations (depolarisations bring the membrane potential closer to the reversal potential of the inward (Na+, Ca++) currents, thus lowering the driving force for inward currents), or due to changes in resistance of the membrane, allowing current to 'shunt' out of the cell without producing the expected depolarisation. Accordingly, sub-linear summation is expected for inputs sufficiently close to eachother on the dendritic tree. However, the passive model of dendritic function is brought into question by several of the studies discussed here, and it is likely that excitatory postsynaptic potentials activate various voltage gated channels (Fricker and Miles, 2000). I firstly discuss the possibility firstly of passive, then active dendritic integration as explanations for the present data.

In the present study, our finding of linear summation suggests several conclusions concerning passive dendritic integration, depending on the location of the different synaptic contacts made by the auditory and visual projections on the deep multi-sensory cells. If the nBIC (auditory) and sSC (visual) projections made synaptic contact on different dendritic branches of their mutual target cell, then the influence of activity in one pathway is unlikely to have interacted directly with that of the other, at least until the arrival of both signals at the soma, or perhaps downstream at a common branching point. As long as the visual and auditory projections did not form

synapses in the same 'local' area, then the responses should not have interacted, and summation should have been linear. On the other hand, if the auditory and visual projections synapsed sufficiently close to one another that driving force and conductance changes were able to affect the summation of post-synaptic potentials, then the linear summation found here might have been the consequence of 'active' dendritic processes (Cash and Yuste, 1998, 1999).

Some support for the former interpretation over the latter can be found here. If active processes were responsible for linear summation, these processes might be voltage-gated, since larger depolarisations would decrease excitatory driving force by a greater amount, and require a larger active compensation. In our study, there was no correlation between membrane potential and the linearity of EPSP summation, suggesting either that voltage-gated mechanisms were not contributing to an active linearity, or that both inward and outward currents were active, the net result being linear summation (Nettleton and Spain, 2000). It could also be that active linearity or supra-linearity may require hyperpolarisation beyond –80 mV, to re-activate voltage-dependent sodium and calcium channels, or increase the driving force for inward currents. Cash and Yuste (1998) reported firstly that linear summation was independent of membrane potential, and secondly that, for small depolarisations linear summation was unaffected by pharmacological blockade, whereas for large depolarisations, blockade of NMDA receptors revealed a potassium channel-mediated sub-linearity. This differentiation between small and large EPSPs was also made for hippocampal neurons by Langmoen and Andersen (1983). For EPSPs larger than 2 mV, sub-linear summation increased with EPSP amplitude. Because the synaptic inputs were well separated (at apical and basal regions), sub-linearity in this preparation was due to the presence of IPSPs, which were eliminated by hyperpolarising the cells to the reversal potential of potassium channels (-85 mV), which are the major source of outward, inhibitory current. All the depolarisations reported in our study (approximately 0.5 – 3 mV) fall within the 'small' categorisation of these studies (Langmoen and Anderson, 1983; Cash and Yuste, 1998), so as long as hippocampal and collicular neurons are similar in how EPSPs are summated, we might not expect to find sub-linearity following pharmacological blockade. It is possible that the depolarisations that we have studied here were insufficiently large to activate currents that boost EPSPs into supra-linearity (Nettleton and Spain, 2000). Further work should address this question, and study the effect of NMDA, AMPA, Na^+, Ca^{++}, and K^+ blockade on EPSP summation.

One caveat that should be mentioned is that supra-linearity *was* found in four cells in the present study, where between 6 and 14 % increases in amplitude occurred with dual stimulation. It could

be that the four cells in which we recorded supra-linear summation were destined to become auditory-visual cells, whereas the remainder were to become auditory-somatosensory, somatosensory-visual, or unimodal. From Wickelgreen (1971) and Wallace and Stein (1997), 57 of 98 and 153 of 405 cells in these two studies respectively, were recorded in the intermediate and deep layers and showed auditory-visual interactions. If these percentages (58 and 38 % respectively) are representative of the true number of auditory-visual cells, then we could expect to find between 3 and 6 cells in the current study that were destined to become auditory-visual cells. However, several other factors have to be taken into consideration. The cells were selected on the basis of their morphology, their ease of obtaining patch-clamp recordings, and the presence of dual monosynaptic inputs. Thus, our sample of cells may be biased if these factors are later found to be important. Auditory-visual cells might be larger, or otherwise easier to patch than other cells, and it might be that purely mono-synaptically connected cells would not receive enough synaptic contacts in order to develop auditory-visual integration. Clearly these issues are important to resolve. An ideal study would examine sub-threshold currents with *in vivo* patch clamp recording and stimulation, to determine which cells respond to auditory and visual stimulation separately or in combination. The technical difficulties of this preparation may preclude the above questions from being resolved – knowledge of the precise position of synaptic inputs onto the dendritic tree may be necessary for reliable conclusions to be drawn (Mel, 1999).

Temporal Independence of Auditory and Visual Events

As with the finding of linear summation, the temporal independence and membrane-potential independence of sub-threshold auditory and visual signals in the deep layer cells suggests either that auditory and visual synaptic contacts are sufficiently distant from eachother to avoid the driving-force and conductance contributions to non-linearity, or that the depolarisations evoked from these dual stimulations are insufficient to bring active processes into play.

The strong paired-pulse homo-synaptic facilitation found in the nBIC projection, and weaker, non-significant facilitation in the sSC projection are probably due to enhancement of pre-synaptic transmission such as increased intracellular calcium (Levitan and Kaczmarek, 1991). This finding is important to confirm that responses to both nBIC and sSC stimuli were capable of being facilitated. Under normal conditions, it may also be important if the normal response to visual and auditory stimuli is a prolonged burst of pre-synaptic activity. Facilitation or potentiation of these synaptic inputs may be critical in the formation of auditory-visual

alignment. Further research should address why the auditory projection from the nBIC shows greater homo-synaptic facilitation than the visual projection.

It is important to know what computational function the multi-sensory cells are performing through development. If these cells are specialised for co-incidence detection, then it is likely that only EPSPs arriving within a narrow temporal window (say, < 5 msec, Nettleton and Spain, 2000) would lead to supra-linearity, whereas if the cells were acting more in an integrate-and-fire mode, the precise timing of EPSPs may be less important. Single unit recording in the cat superior colliculus provides interesting food for thought on this question. Wallace and Stein (1997) found that in the first five weeks of life, only auditory and visual stimuli that occurred simultaneously led to multi-sensory enhancement in the cat. At seven weeks, visual stimuli could precede auditory stimuli by 100 msec, and in the adult by 300 msec, and still lead to enhancement in the number of action potentials fired per presentation. Similarly, an earlier study (Meredith *et al*., 1987) found that, in adult cats, signals from different modalities were integrated over a long temporal window, which enables animals to detect coincident auditory-visual information over a much wider spatial extent. In the anaesthetised guinea-pig SC, King and Palmer (1995) found that visual stimuli had to precede auditory stimuli by 50 – 80 msec in order for multi-modal enhancements or depression to occur. This temporal offset may either be compensated for by transduction and conduction latency differences, or the visual response must be prolonged in order that multi-sensory enhancement can occur.

These studies suggest that, early in development, precise stimulus timing may be of utmost importance, and later, as visual and auditory projections mature there is a much larger window for temporal integration, and hence a potentially more dynamic and useful orienting repertoire. The data reported here do not suggest that auditory-visual coincidence detection relies on a specific sub-threshold mechanism. Rather, multi-sensory enhancement and map alignment is more likely due to supra-threshold synaptic plasticity.

What are the Mechanisms of Visual Guidance?

How is the alignment of visual and auditory topographies brought about? The present results do not support the possibility of a sub-threshold active ‘boosting’ mechanism that is brought into play when EPSPs from both auditory and visual pathways occur simultaneously or within 150 msec of eachother. More likely, visual responses guide the auditory topography though a supra-threshold mechanism, probably involving long-term potentiation of auditory synaptic activity. If EPSPs elicited by auditory stimulation coincided with a visually-evoked depolarisation of the

multi-sensory cell, then the auditory projection might show long-term potentiation. Stimulation of the superficial layers of the superior colliculus often produces a sequence of excitatory post-synaptic currents in the deep layer cells, which can outlast the initial stimulus by 100-fold (Lee *et al*., 1997), and lead to action potential firing. This kind of post-synaptic activity, Lee and colleagues (1997) noted, was similar in duration to the normal bursting properties of many collicular pre-motor neurons. If the auditory pathway were also active during this visually-evoked bursting activity, then potentiation of auditory synapses onto this cell might occur.

The precise timing of auditory and visual activity may be important. As mentioned above, Wallace and Stein (1997) found a much greater sensitivity for auditory and visual stimulus timing in new-born cats compared to adults, in order for multi-sensory enhancement to occur. Neurons in the younger cat's SC preferred simultaneous activity, and in the adult cats, visual stimuli could precede auditory by up to 300 msec. A recent report (Feldman, 2000) demonstrated timing-based LTP and LTD in somatosensory cortex synapses in the rat. He found that the temporal window for long-term potentiation induction was less than 50 msec (being the maximum time after an EPSP on a given cell, that an action potential must arrive to potentiate the synapse responsible for the EPSP). Outside of this window, long-term depression, or no synaptic plasticity occurred. In terms of the present study, it may be that auditory EPSPs depolarise a multi-sensory cell that is already slightly depolarised, or that is co-incidentally depolarised by visual activity from the superficial layer projection, or indeed other visual projections, and push the membrane potential above action potential threshold. This might allow the auditory projection synapses that align with the topographic visual projection to be strengthened, and non-aligning auditory signals to be weakened. There may thus be quite a short temporal window within which auditory and visual synaptic interaction or integration must occur.

An important factor to take into consideration is that the presence of visual activity in deep, multi-sensory cells may not occur until a late stage in development. In the cat, deep-layer visual responses begin at quite a late stage (Wallace and Stein, 1997). Somatosensory responses are present from birth, auditory responses follow after 12 weeks, and from the 20th week visual responses are observed. Remarkably, when multi-sensory enhancement first occurs (at 5 weeks for auditory-somatosensory stimuli), it is at adult levels: it is the proportion of cells that display multi-sensory enhancement that increase, not the extent to which each cell displays the enhancement. These developmental phenomena suggest that whatever process is guiding the development of multi-sensory convergence and enhancement, it is either a process occurring

below the threshold for detection of reliable single-unit responses to visual stimulation, or that the vital entrainment period is very brief. Wallace and Stein (1997) studied one animal at 15, one at 17, and one at 20 days post-natal. So the critical auditory-visual plasticity must occur and be complete within at most 5 days, allowing for individual variation. The development of multi-sensory integration in the rat superior colliculus remains to be studied, but it would certainly be beneficial to know at what developmental stage visual and auditory responses, and multi-sensory enhancement are first seen.

Where is the Primary Site of Visual-Guidance?

The superior colliculus receives auditory projections from both the nBIC and the external nucleus of the inferior colliculus (ICX). This latter projection is weaker than the projection studied here, but there are several reports that suggest its role in audio-visual plasticity is important. Feldman and Knudsen (1997) placed prisms on juvenile barn owls, which displaced their visual field by 23º to the left or right. They found that the inter-aural time difference (ITD) tuning of optic tectum (the homologue of the mammalian superior colliculus) neurons and ICX neurons was shifted by the abnormal visual experience, but not neurons within a nucleus earlier in the auditory pathway, the lateral shell of the central inferior colliculus nucleus (ICC-ls). Neuroanatomical tract-tracing showed that the projection onto ICX neurons which previously would have represented normal ITD tuning values, was enlarged, such that more cells from a wider range of ICC-ls locations were now contributing to the ICX's response. Conversely, no change in ICX or optic tectum tuning was observed. This result suggests that auditory map plasticity as recorded in the optic tectum (or SC) may be the result of plasticity at an earlier processing stage, or indeed, there may be no plasticity in the optic tectum or SC at all.

The projection from the nucleus of the brachium of the inferior colliculus to the superior colliculus may not be the critical auditory projection involved in visual guidance. Schnupp and King, (1997) speculated that because of the weak topography in the nBIC, other auditory projections may be required in order for auditory topography to develop under visual guidance. The ICX projection to the SC may be such a candidate for aiding visual guidance. If ITD tuning in this nucleus is altered mainly by alterations in the projection it receives from the central nucleus of the inferior colliculus (Feldman and Knudsen, 1997), then it may be a better, i.e. more topographical, template *via* which the nBIC-SC topography can develop. Furthermore, the nBIC receives a back-projection from the SC, in which some visual responses are observed (Doubell *et al*., 2000). Further work on this question should study the facilitation of EPSPs evoked by ICX, SC and nBIC stimulation, and their inter-relations.

Conclusion

If the alignment of auditory and visual maps in the superior colliculus is dependent on a sub-threshold mechanism in layer IV multi-sensory cells, then this mechanism may be cell-type specific, and the present study may not have been sensitive enough to isolate those units responsible. Alternatively, the guidance of auditory topography may be due to supra-threshold mechanisms whereby auditory synapses coincidentally active with strong visually-evoked depolarisations of the same cell are potentiated. Finally, it might be that the site of visual guidance of the auditory map in the superior colliculus is not in the superior colliculus, but at an earlier processing stage, probably in the inferior colliculus. Definitive answers to these questions will have important implications for understanding the experience-dependent mechanisms of the development of neuronal connectivity throughout the brain, not just in the alignment of multi-sensory spatial maps in the mammalian superior colliculus.

References

Brainard MS, Knudsen EI (1998) Sensitive periods for visual calibration of the auditory space map in the barn owl optic tectum. *Journal of Neuroscience* **18**:3929-3942

Cash S, Yuste R (1998) Input summation by cultured pyramidal neurons is linear and position-independent. *Journal of Neuroscience* **18**:10-15

Cash S, Yuste R (1999) Linear summation of excitatory inputs by CA1 pyramidal neurons. *Neuron* **22**:383-394

Doubell TP, Baron J, Skaliora I, King AJ (2000) Topographical projections from the superior colliculus to the nucleus of the brachium of the inferior colliculus in the ferret: convergence of visual and auditory information. *European Journal of Neuroscience* **12**:4290-4308

Feldman DE (2000) Timing-based LTP and LTD at vertical inputs to layer II/III pyramidal cells in rat barrel cortex. *Neuron* **27**:45-56

Feldman DE, Knudsen EI (1997) An anatomical basis for visual calibration of the auditory space map in the barn owl's midbrain. *Journal of Neuroscience* **17**:6820-6837

Ferster D, Jagadeesh B (1992) EPSP-IPSP interactions in cat visual cortex studied with in vivo whole-cell patch recording. *Journal of Neuroscience* **12**:1262-1274

Fricker D, Miles R (2000) EPSP amplification and the precision of spike timing in hippocampal neurons. *Neuron* **28**:559-569

Harris LR, Blakemore C, Donaghy M (1980) Integration of visual and auditory space in the mammalian superior colliculus. *Nature* **288**:56-59

King AJ (1999) Sensory experience and the formation of a computational map of auditory space in the brain. *BioEssays* **21**:900-911

King AJ, Carlile S (1993) Changes induced in the representation of auditory space in the superior colliculus by rearing ferrets with binocular eyelid suture. *Experimental Brain Research* **94**:444-455

King AJ, Palmer AR (1983) Cells responsive to free-field auditory stimuli in guinea-pig superior colliculus: distribution and response properties. *Journal of Physiology* **342**:361-381

King AJ, Palmer AR (1985) Integration of visual and auditory information in bimodal neurones in the guinea-pig superior colliculus. *Experimental Brain Research* **60**:492-500

King AJ, Hutchings ME, Moore DR, Blakemore C (1988) Developmental plasticity in the visual and auditory representations in the mammalian superior colliculus. *Nature* **332**:73-76

King AJ, Jiang ZE, Moore DR (1998a) Auditory brainstem projections to the ferret superior colliculus: Anatomical contribution to the neural coding of sound azimuth. *Journal of Comparative Neurology*, **390**:342-365

King AJ, Schnupp JWH, Thompson ID (1998b) Signals from the superficial layers of the superior colliculus enable the development of the auditory space map in the deeper layers. *Journal of Neuroscience* **18**:9394-9408

King AJ, Parsons CH, Moore DR (2000) Plasticity in the neural coding of auditory space in the mammalian brain. Proc*eedings of the National Academy of Sciences, USA* **97**:11821-11828

Knudsen EI (1998) Capacity for plasticity in the adult owl auditory system expanded by juvenile experience. *Science* **279**:1531-1533

Knudsen EI, Brainard MS (1991) Visual instruction of the neural map of auditory space in the developing optic tectum. *Science* **253**:85-87

Langmoen IA, Andersen P (1983) Summation of excitatory postsynaptic potentials in hippocampal pyramidal cells. *Journal of Neurophysiology* **50**:1320-1329

Larkum ME, Launey T, Dityatev A, Lüscher H (1998) Integration of excitatory postsynaptic potentials in dendrites of motoneurons of rat spinal cord slice cultures. *Journal of Neurophysiology* **80**:924-935

Lee PH, Helms MC, Augustine GJ, Hall WC (1997) Role of intrinsic synaptic circuitry in collicular sensorimotor integration. *Proceedings of the National Academy of Sciences, USA* **94**:13299-13304

Levitan IB, Kaczmarek LK (1991) *The Neuron: Cell and Molecular Biology*. Oxford University Press, Oxford

Mel BW (1999) Why have dendrites? A computational perspective. In Stuart G, Spruston N, Häusser M. (eds.) *Dendrites*, Oxford University Press, Oxford, p 271-289

Meredith MA, Nemitz JW, Stein BE (1987) Determinants of multisensory integration in superior colliculus neurons. I. Temporal factors. *Journal of Neuroscience* **7**:3215-3229

Nettleton JS, Spain WJ (2000) Linear to supralinear summation of AMPA-mediated EPSPs in neocortical pyramidal neurons. *Journal of Neurophysiology* **83**:3310-3322

Schnupp JWH, King AJ (1997) Coding for auditory space in the nucleus of the brachium of the inferior colliculus in the ferret. *Journal of Neurophysiology* **78**:2717-2731

Schnupp JWH, King AJ, Smith AL, Thompson ID (1995) NMDA-receptor antagonists disrupt the formation of the auditory space map in the mammalian superior colliculus. *Journal of Neuroscience* **15**:1516-1531

Skaliora I, Doubell TP, Alli A, King AJ (2002) Converging visual and auditory inputs to single cells in the deep layers of the superior colliculus. *Poster presented at FENS*, Paris, 2002

Stein BE, Magalhães-Castro B, Kruger L (1975) Superior colliculus: Visuotopic-somatotopic overlap. *Science* **189**:224-226

Tamás G, Szabadics J, Somogyi P (2002) Cell type- and subcellular position-dependent summation of unitary postsynaptic potentials in neocortical neurons. *Journal of Neuroscience* **22**:740-747

Wallace MT, Stein BE (1997) Development of multisensory neurons and multisensory integration in cat superior colliculus. *Journal of Neuroscience* **17**:2429-2444

Wickelgreen BG (1971) Superior colliculus: Some receptive field properties of bimodally responsive cells. *Science* **173**:69-73

Wolf E, Zhao F, Roberts A (1998) Non-linear summation of excitatory synaptic inputs to small neurones: a case study in spinal motoneurons of the young *Xenopus* tadpole. *Journal of Physiology* **511**:871-886